Journal of Molecular Modeling (2024) 30:51
https://doi.org/10.1007/s00894-024-05842-2

ORIGINAL PAPER

Structure-based drug design and molecular dynamics studies of an allosteric modulator targeting the protein–protein interaction site of PDK1

Vennila Kailasam Natesan[1] · **Elango Kuppannagounder Pitchaimuthu**[1]

Received: 7 July 2023 / Accepted: 9 January 2024 / Published online: 26 January 2024
© The Author(s), under exclusive licence to Springer-Verlag GmbH Germany, part of Springer Nature 2024

Abstract

Context Protein–protein interaction interfaces play a major role in cell signaling pathways. There is always a great interest in developing protein–protein interaction (PPI) inhibitors of kinases, as they are challenging due to their hydrophobicity, flat surface, specificity, potency, etc. 3 Phosphoinositide-dependent kinase-1 (PDK1), which is involved in the PI3K/PDK1/AKT pathway, is a cancer target that has gained insight for the past two decades. PDK1 possesses a protein interaction fragment (PIF) pocket, which is a well-known PPI that targets allosteric modulators. This work focusses on energy-based pharmacophore model development which on virtual screening could yield novel scaffolds towards the drug designing objective for the kind of PDK1 modulators. A novel pyrazolo pyridine molecule was identified as an allosteric modulator that binds to the PPI site. The metadynamics simulations with free energy profiles further revealed the conformational allosteric changes stimulated on the protein structure upon ligand binding. The cytotoxic activity (IC_{50}-20 μM) of the identified compound against five different cancer cell lines and cell cycle analysis supported the anticancer activity of the identified compound.

Methods All the computational works were carried out by the most commonly used Schrodinger Suite software. The pharmacophore was validated by Receiver Operation Characteristics (ROC) and screening against allosteric Enamine database library. The Optimized Potential Liquid Simulations (OPLS-2005) was used to minimize the structures for molecular docking calculations, and inbuilt scoring method of ranking the compounds based on docking score and Glide energy was used. Molecular dynamics simulations were conducted by Desmond implemented in Maestro. The hit compound was purchased from Enamine and tested against different cancer cell lines by MTT assay, apoptosis by western blotting technique, and by flow cytometry analysis.

Keywords Allosteric modulator · Hotspot-based pharmacophore · Virtual screen · Phosphoinositide-dependent kinase · Metadynamics simulations

Introduction

Protein–protein interaction (PPI)-based drug discovery is currently emerging with remarkable advances over the past two decades. PPIs play a fundamental role in all life events and cellular activities, regulating apoptosis and mediating various biochemical reactions, such as signal transduction and metabolism. It is estimated that there are approximately 650,000 types of specific protein–protein interactions in a human cell [1]. Due to biophysical and biochemical limitations in cancer cells, targeting PPIs with small molecules or peptides remains a difficult task for academia as well as the pharmaceutical industry. Usually, the PPI site in proteins is wide and flat, more hydrophobic, large in surface area, challenging to target with small molecules, and not always druggable. However, the idea of "hotspots", the residues lining the PPI site that contribute energetically high in interacting with other proteins, changes the situation to an alternative way of developing the allosteric modulators of PPI [2–5]. Either the activator that binds at the PPI site that stimulates the intrinsic activity of the enzyme but disrupts the interaction with other proteins or the inhibitor that binds with the PPI site and allosterically affects the enzyme's activity leads to therapeutic development strategies.

✉ Vennila Kailasam Natesan
vennilakn@gmail.com

[1] The Gandhigram Rural Institute-Deemed to be University, Tamilnadu 624302, India

Several approaches have been used to develop PPI modulators in recent years, such as pharmacophore modeling [6], fragment-based drug design [7], NMR-based fragment screening, molecular dynamics simulations, and competitive binding assays. Enasidenib was first developed in silico as a selective allosteric inhibitor of the tumor target, IDH2. Nutlins are the first class of MDM2 inhibitors mimicking the p53 peptide identified by SPR-based competitive assays [8]. Venetoclax [9] is considered the first FDA-approved BH3-mimetic drug to interfere with PPIs, identified by fragment-based drug discovery.

3-Phosphoinositide-dependent kinase-1 (PDK1) was chosen for the present work because it is a well-studied enzyme and a well-known cancer target. The constitutive activation of the enzyme due to oncogenic mutation initiates tumorigenesis [10–12]. The inhibitor design pointing at the ATP binding site led to off-target effects due to the presence of conserved residues at the active site of similar kinases. The alternative strategy is to target other sites of PDK1, as it has three different binding sites. It has been biochemically proven that it interacts with four substrate proteins, namely, S6K1, SGK1, PKC-ζ, and PKC-related kinase-2 (PRK2), through the PIF pocket [13, 14]. The hydrophobic motif present in the small lobe of PDK-1 lined by the residues Lys115, Ile118, and Ile119 on the αB-helix, Val124, and Val127 on the αC-helix and Leu155 on β-sheet 5 forms a 5 Å deep pocket known as the PIF pocket, which acts as the docking site for the substrates. Among the mentioned residues, Leu155 is the key residue that inhibits the PDK1 interaction with other proteins. The PIF pocket residues Lys115, ILE118, Ile119, Val124, and Val127 upon mutation reduce the tenfold affinity of the PDK1 interaction. PDK1 was also found to recruit, phosphorylate, and activate 23 other AGC kinases, including AKT, S6K, SGK, RSK, and PKC isoforms, which regulate cell survival, proliferation, and metabolism [15, 16]. This type of PDK1 binding with physiological substrate proteins can be recognized as protein–protein interactions (PPIs), and the interface is a known PPI site [17]. This PDK1 protein–protein interface possesses a secondary structure epitope and has proven to be druggable [4]. The PPI interaction in the case of PDK1 is a phosphorylation-dependent mechanism, as it has a phosphate binding site that activates PDK1 binding only after phosphorylation of the substrates and allosterically activates PDK1 kinase activity [17]. These types of interactions involve large conformational changes enabling the inactive-active conformational transition of PDK1 through the regulatory site.

Thus, targeting this PPI site may endow modulators that either activate or inhibit the regulation of PDK1 function. One of the strategies for inhibiting the recruitment of such substrates by PDK1 is to develop small compounds that bind the PPI site, thereby modulating the binding [16, 18–20]. Small molecule activators, when bound to PDK1, disrupt PDK1-substrate binding and allosterically regulate the catalytic activity of the enzyme. A small molecule occupying a limited space in the HM/PIF pocket defined by Ile119, Leu155, Val127, and Arg131 was able to activate PDK1 [18]. The hydrogen bonding interactions of small compounds with residues Arg131 and Gln150 established by the amide group, Tyr126 movement away from the active site, and the disordered αB and αC helices gave rise to an allosteric inhibitor [21]. Hence, there is always significant interest in identifying allosteric modulators [4, 22–26]. It is also predicted that the potential for developing new types of kinase inhibitors is huge, and it will continue to be a major growth area over the next 20 years [27].

In this study, screening of a small library of 4800 allosteric kinase inhibitors yielded a pyrazole pyridine derivative with structural and functional impacts on PDK1. The pharmacophore hypothesis developed based on the energy of the hotspots is screened against a small library of allosteric compounds, and the results are discussed. The binding nature of the identified hit molecule was further validated using molecular docking and free energy analysis by metadynamics simulations whose main purpose was to explore the nature of allosteric interactions required for diagnostic agents to bind within the PDK1 protein–protein interface. The biological activity of the identified compound with five different cancer cell lines and cell cycle analysis is also presented.

Experimental

Structure-based design

The three-dimensional coordinates of 3 phosphoinositide-dependent kinase-1 bound with PIFtide (a peptide substrate) were downloaded from the Protein Data Bank (PDB ID: 4RRV). The protein was prepared with the Protein preparation module in Schrodinger. The missing residues in the crystallographic structure were built with Prime in Maestro, and the hydrogens were added. The structure was optimized by the OPLS2005 forcefield, and the structure was refined for added hydrogens. The pharmacophore model was developed by generating pharmacophores in the Phase module [28] in Schrodinger Suite 2017 [29]. The developed model was validated using decoys generated from the Schrodinger decoys database. The potential PIF pocket binders cocrystallized with PDK1 and whose three-dimensional structures were deposited in PDB were considered actives. The pharmacophore hypothesis was validated with the receiver operation characteristic curve. The validated pharmacophore was then screened against the Enamine allosteric compound library by phase ligand screening. The resulting hits were subjected to virtual

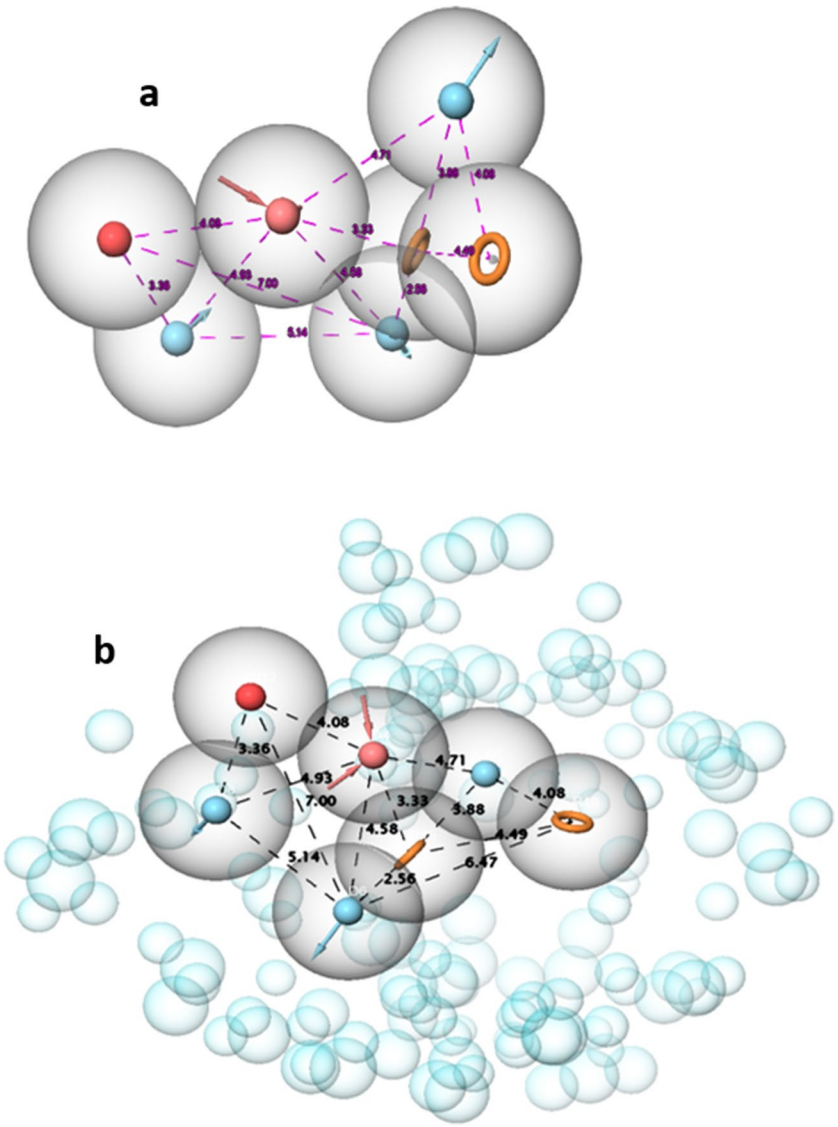

Fig. 1 **a**. Seven featured pharmacophores (NDDDARR) created from hotspots with three Hbond donors (blue sphere with arrows), two aromatic rings, one Hbond acceptor (peach sphere with arrow), and a negatively charged interaction (orange sphere). **b**. Excluded volumes with blue transparent spheres based on 4RRV. (The excluded volumes on the second cavity of the ATP site are omitted for clarity)

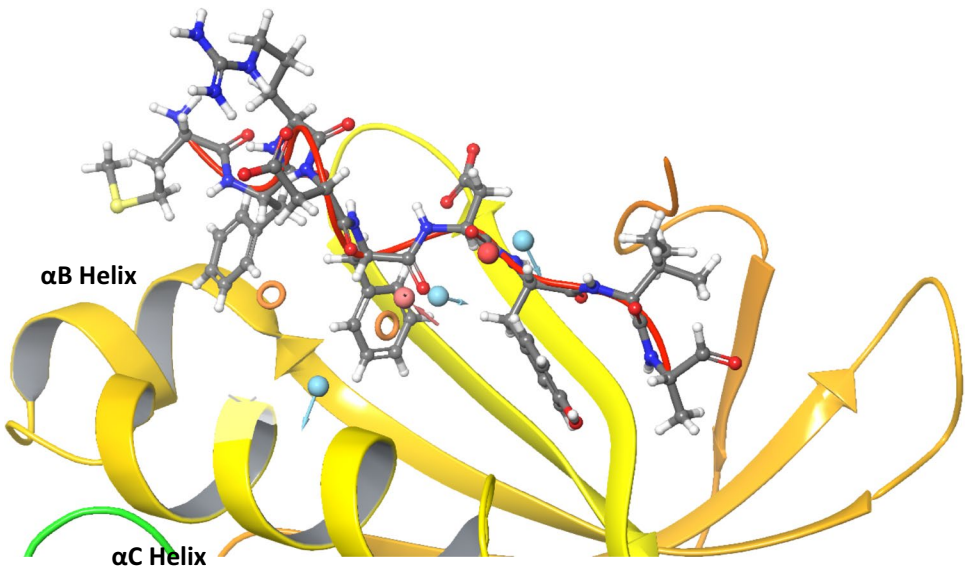

Fig. 2 The alignment of pharmacophore model features with PIFtide cocrystallized PDK1 (PDB ID: 4RRV), where PIFtide is shown as a red ribbon with their side chains represented as gray sticks

screening workflow algorithms implemented in the Maestro interface. The refined hit receptor–ligand complex was chosen for metadynamics simulations

Metadynamics simulations

The docked pose will not always result in the exact interactions between receptors and ligands, and to mimic the protein–ligand binding event in an actual solvated environment and to trace its conformational transition pathway, metadynamics simulations were carried out. The Desmond interface developed by D.E. Shaw Research group [30] implemented in Maestro on the Ubuntu Linux platform in the HPZ238 workstation served this purpose. The best pose of the docked PDK1- Z1147972667 was solvated with a TIP4P water model in an orthorhombic box and neutralized by 0.15 M NaCl. The prepared complex was minimized by the Optimized Potential for Liquid Simulations (OPLS2005) forcefield. The two collective variables CV1 (αB helix length) and CV2, hinge distance (distance between Gly rich loop and ASP 205). Metadynamic parameters such as height (0.03 kcal/mol), interval (0.09 ps), temperature (300 K), and pressure (1 bar) were used as default, and the model system was relaxed before simulation. The production run of the simulation was carried out for 200 ns of the ensemble class as the NPT, and the trajectory was recorded at every 200 ps interval; therefore, 1000 frames of trajectory were collected. The RMSD and RMSF were determined for each frame with respect to frame 1 throughout 200 ns of simulation time. The number of hydrogen bonds and other nonbonding interactions throughout the simulation time was calculated. The free energy surface diagram was obtained by the metadynamics analysis module in Desmond.

MTT assay

The hit compound was purchased from Enamine (Product No: Z1147972667, N-{5-[(3-fluorophenyl)methyl]-1,3,4-thiadiazol-2-yl}-3,6-dimethyl-1H-pyrazolo[3,4-b]pyridine-4-carboxamide, 90%) and used for cytotoxic assays. The compound was dissolved in DMSO to prepare stock solution and diluted with PBS at pH 7.2 for working solution. The MTT (3-(4,5-dimethylthiazol-2-yl)-2,5-diphenyltetrazolium bromide) assay was carried out against PC-3, LNCaP, and DU145 prostate cancer cells as well as Hep3B, SiHa, and HeLa cancerous cell lines. The cells were obtained from the American Type Culture Collection and cultured in DMEM (Dulbecco's Modified Eagle's Medium) supplemented with 10% FBS and 1% antibiotic (Welgene, South Korea). The cells were seeded onto 96-well plates, and the compound was added at different dilutions and incubated for 24 h.

Cell cycle analysis

PC3 and LNCaP cells (1×10^6cells/ml) were treated with 0,40, and 80 μM concentrations of the hit compound and were subjected to cell cycle analysis using FACS Calibur (Becton Dickinson, Franklin Lakes, NJ) using CellQuest Software. The procedures were followed as reported [31]. All statistical analyses were carried out by Sigmaplot 12.0, and the data are expressed as the means ± SDs.

Results and discussion

Hotspot-based pharmacophore generation

The three-dimensional coordinates of 3 phosphoinositide-dependent kinase-1 bound with PIFtide (a peptide substrate) were downloaded from the Protein Data Bank (PDB ID: 4RRV). The protein was prepared with the Protein preparation module in Schrodinger. The missing residues in the crystallographic structure were built with Prime in Maestro, and the hydrogens were added. The structure was optimized by the OPLS2005 forcefield, and the structure was refined for added hydrogens. The pharmacophore model was created using the hotspot residues of PDK1 that are involved in the interactions with the PIFtide substrate of PDK1, namely, Lys76, Val127, Arg131, Tyr146, Thr148, Gln150, Phe157, and Leu155. The resulted seven-feature model (NDDDARR) with excluded volumes shown in Fig. 1a has two aromatic rings represented by letter R, three H bond donors denoted by letter D, one H bond acceptor with letter A, and a negative ionizable bond represented by the letter N. Among the excluded volumes, two cavities (ATP site and

Table 1 The hit molecules from the virtual screen workflow with their critical parameters

S. No	Catalog ID	ClogP	Number of sites matched	Phase screen score	Glide gscore[a]
1	Z1147972667	3.117	4	0.375	−4.519
2	Z1185766474	2.991	4	0.406	−4.886
3	Z809380814	3.309	4	0.467	−4.835
4	Z340588958	1.806	4	0.479	−4.883
5	Z1603709568	2.52	5	0.382	−4.694
6	Z220356320	2.382	4	0.459	−4.736
7	Z1834079437	3.043	4	0.437	−4.645
8	Z88897443	2.509	4	0.376	−4.556
9	Z52997366	1.552	5	0.432	−4.53
10	Z56926818	2.415	4	0.396	−4.54
11	Z1355941678	2.552	4	0.428	−4.915
12	Z1673510588	1.876	4	0.417	−4.874

[a]In kcal/mole

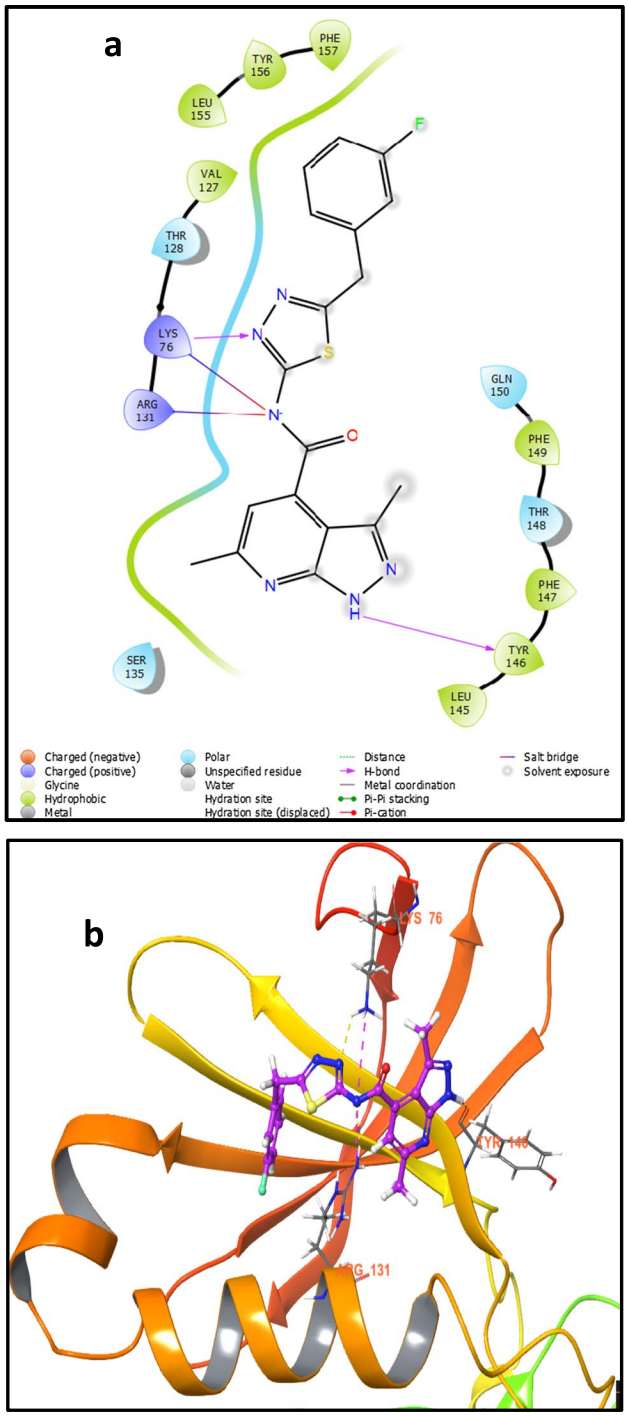

Fig. 3 **a**. The receptor–ligand interaction of compound Z1147972667 with PDK1 residues. **b**. Ligand occupancy in the PPI docking site and interactions with Lys76, Arg131, and Tyr146 as dashed lines

PIF pocket) were observed, and the excluded volumes generated along with the pharmacophore that corresponds to the protein–protein interface were used for pharmacophore screening (Fig. 1b).

Pharmacophore model validation

The obtained pharmacophore features generated from hotspot residues were overlaid with the PPI region of PDK1, and interestingly, the aromatic ring feature was well aligned with the phenyl ring of Phe 17, Hbond Acceptor with the carbonyl backbone of Phe17, and another H-bond donor and negative charge with peptide bonds of ASP18 of PIFtide (Fig. 2). Hence, these features can serve as authentication to utilize them for further ligand matching. The pharmacophore generated must be evaluated to ascertain its quality. The pharmacophore model was validated by ligand screening of 84 compounds, including four actives and eighty decoys (Fig. S1) generated from Glide Drug-like Ligand Decoy sets. Interestingly, the created pharmacophore model picked up one active compound without any false positives, which corresponds to an enrichment of (1/1) ÷ (1/84) ≈83.33. The ROC curve obtained for the hypothesis (Fig. S2) in which the curve pointing on the left side of the diagonal of false positives proved the hypothesis to be good with area under ROC curve score of 0.82.

Dataset generation and pharmacophore screening

The developed model was then utilized to screen the enamine allosteric library that contains 4800 compounds. All compounds were prepared using Ligprep in Maestro by generating conformers before screening. All seven features with excluded volumes were included for screening, and partial matches of the pharmacophoric points were allowed with criteria of matching at least four points without any constraints.

Molecular docking-based virtual screening

The 1000 hits generated as output were used in the virtual screening workflow, including the high throughput virtual screen mode, and the top ten percent of the hits were subjected to simple precision docking. The top ten percent of the SP results were fed to extra precision (XP) docking, and the hit results were obtained with 12 compounds (Table 1). The manual inspection of ligand interactions of all the compounds inferred that compound Z1147972667, which has a glide gscore greater than −4.5, possesses more hydrogen bonds with key residues (Fig. S3). To be an allosteric modulator for the PIF pocket, the compound must possess a carboxylate group, i.e., a negative charge, but in this case, the nitrogen atom in the peptide bond becomes deprotonated and thus provides a negative charge to the ligand molecule. Two salt bridges with a deprotonated nitrogen atom and Lys76 and Arg131 and two hydrogen bonds with nitrogen atoms in five-membered ring systems and Tyr156 and Lys76 stabilize

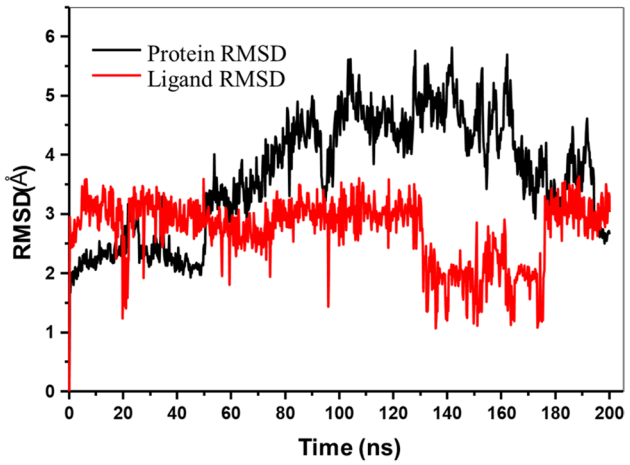

Fig. 4 Protein and ligand RMSD plotted against the simulation time

the molecule in the PPI region with a binding energy of −4.519 kcal/mol (Fig. 3).

Molecular dynamics simulations

The binding stability of the receptor–ligand complex, intermolecular interactions, and conformational changes of the structure can be derived from molecular dynamics simulations. Although the molecular docking results have given out the intermolecular interactions where the solvent effect is neglected, it is more reliable to consider the solvent effects and the molecular motions with respect to temperature and pressure. Molecular dynamics simulations will handle those situations in the molecular environment to move close to reality. The receptor–ligand complex of PDK1- Z1147972667 was initially predefined with 9613 TIP3P water molecules to constitute the orthorhombic system of length 10 Å with 33581 atoms altogether; 0.15 M NaCl was added, and the OPLS2005 forcefield was applied to set up the system in which energy was minimized. After energy minimization, seven stages were executed to relax the system as per the default settings in Desmond. The relaxed system was submitted to 200-ns MD simulation, carried out under the NPT ensemble using a Nose–Hoover thermostat at 300 K and Martyna-Tobias-Klein barostats at 1.01325 bar pressure [32]. A snapshot of the simulated structure was recorded every 200 ps, and energy was recorded every 1.2 ps.

Thousand frames were collected over 200 ns, and the root mean square fluctuations, root mean square deviation, protein–ligand interaction, and energy potential were acquired. The root mean square deviation (RMSD) measured the average change in displacement of a selection of atoms (protein/ligand) for a particular frame concerning the first reference frame. The RMSD evolution of the protein above 5 Å gives us insight into the conformational change of the protein backbone during simulation. From Fig. 4, it can be noted that the RMSD increases initially up to 100 ns and gradually decreases and reaches below 3.2 Å at the end, which indicates that the protein structure is regaining its initial state after reaching equilibrium. These pronounced conformational changes might arise due to ligand binding and its allosteric effect on the protein structure. RMSF values characterize the local changes along the protein chain. The RMSF plot consists of peaks that indicate areas of the protein that fluctuate the most during the simulation. The αB helix fluctuates more, i.e., > 5 Å, and the αC helix fluctuates to 3 Å, which indicates that the ligand influences the motion of both the helices as well as the T-loop (Fig. 5).

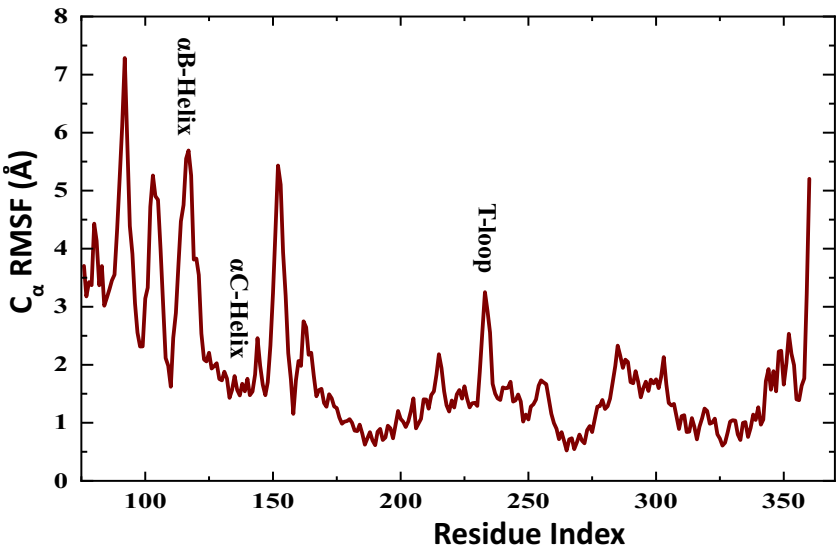

Fig. 5 Root mean square fluctuations (RMSF) of the protein residues during simulation depicting more conformational changes in the αB helix region

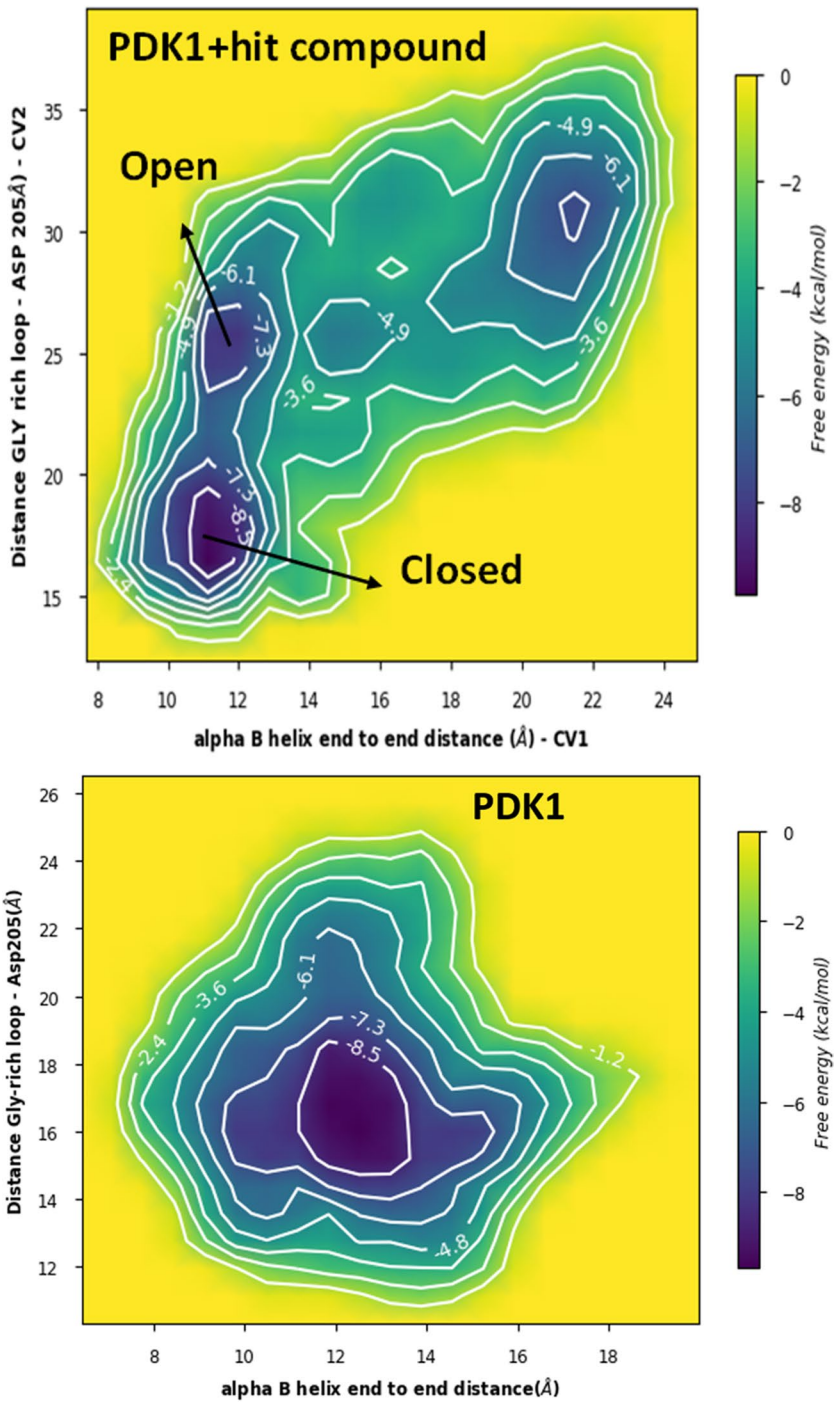

Fig. 6 The free energy landscape from metadynamics simulations of PDK1 with ligand and without ligand with distinct energy minima shows that the ligand has stabilized PDK1 in an open inactive form in its conformational transition pathway

Free energy surface analysis

Conventional molecular dynamics is not very efficient in analyzing complete conformational changes, and hence, few enhanced sampling methods, such as metadynamics, umbrella sampling [33, 34], and multiple replicas in parallel tempering methods [19], are being used by researchers. Thus, the metadynamics simulations of PDK1-Z1147972667 were performed in Desmond, and the free energy surfaces were reconstructed using two collective variables (CV): CV1, αB helix end-to-end distance, and CV2, the distance between Gly rich loop and Asp205, which describes the kinase hinge motion. Three energy minima (−7.5 to −9.8 kcal/mol) were calculated in which one of the minima (Fig. 6) is well populated with closed structures with hallmark salt bridge between Lys111-Glu130 and hinge distance < 20 Å and other minima with open structures of hinge distance > 25 Å without the salt bridge. Additionally,

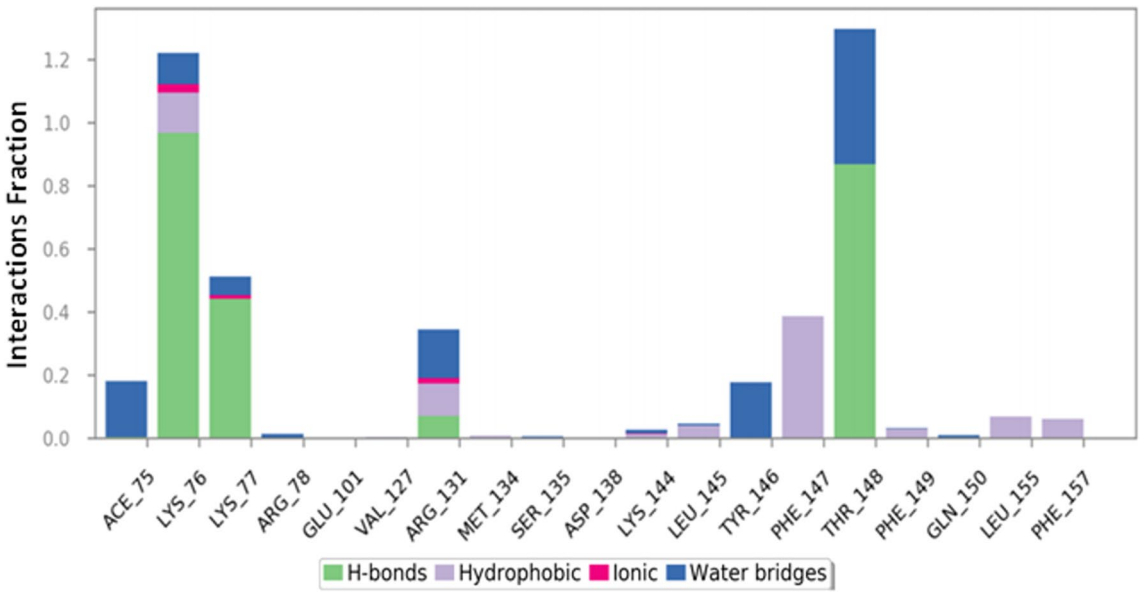

Fig. 7 Contribution of protein–ligand interactions to the binding event showing all the previously reported amino acid residues involved in binding with the ligand

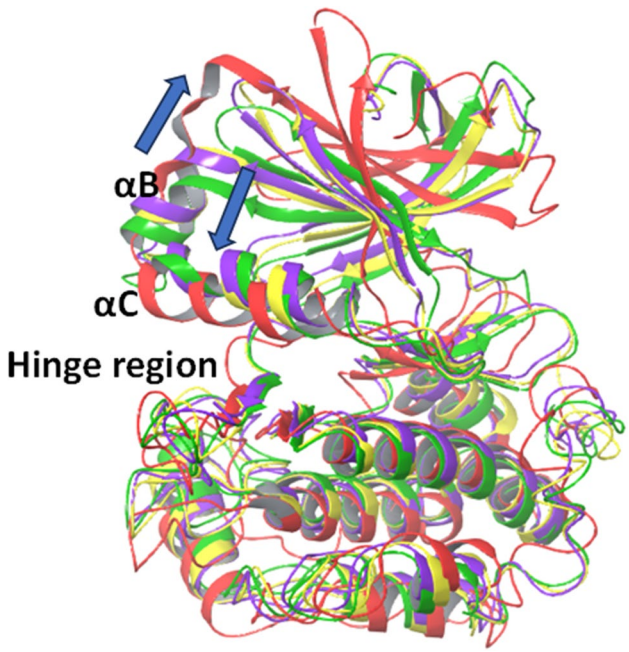

Fig. 8 The superimposition of representative structures from four clusters indicating the upward αB helical movement and αC helix moving downward (indicated by blue arrows) and can be viewed in orange-colored conformation with the opening of the loop in the hinge region

the diffusive CVs can represent the convergence and thereby the stability of the system. From Fig. 6, we can see the well-diffused CVs beyond −3.6 kcal/mol, which indicates convergence of the simulation.

This free energy landscape with the lowest energy of −8 to −9.8 kcal/mol discriminates the equilibrium transition between the open and closed states of PDK1 upon ligand binding. In addition to these two minima, the third one also corresponds to an open structure but with a highly disturbed N lobe and unwind αB helix. However, in the similar metadynamics simulation of PDK1 without any ligand in the PIF pocket (Fig. 6), the free energy mapping consists of only one energy minimum representing the closed active conformation.

Allosteric mechanism

Similar to the PIFtide interaction, the ligand interacts with Arg131 and Thr148, water-mediated interactions with Arg131, Thr146, Thr148, Glu150, and hydrophobic interactions with Phe147, Phe149, Leu155, and Phe157, which are the key amino acid residues involved in substrate docking (Fig. 7). The occupancy of the ligand in the PPI site influences the movement of the αC helix as well as the hydrophobic interactions formed between the aromatic amino acid residues in the PPI site and the ligand. The ionic interactions formed between the negatively charged nitrogen atom of the ligand and Arg131 played critical roles in ligand binding, as observed from experiments with other allosteric modulators. [14, 35] The salt bridge with Arg131 implies strong binding affinity, as reported in PS210 [36]. The obtained trajectory frames were clustered based on RMSD by the average hierarchical cluster linkage method, and representative structures from each cluster were superimposed to view the differences in the conformation (Fig. 8). The more deviated

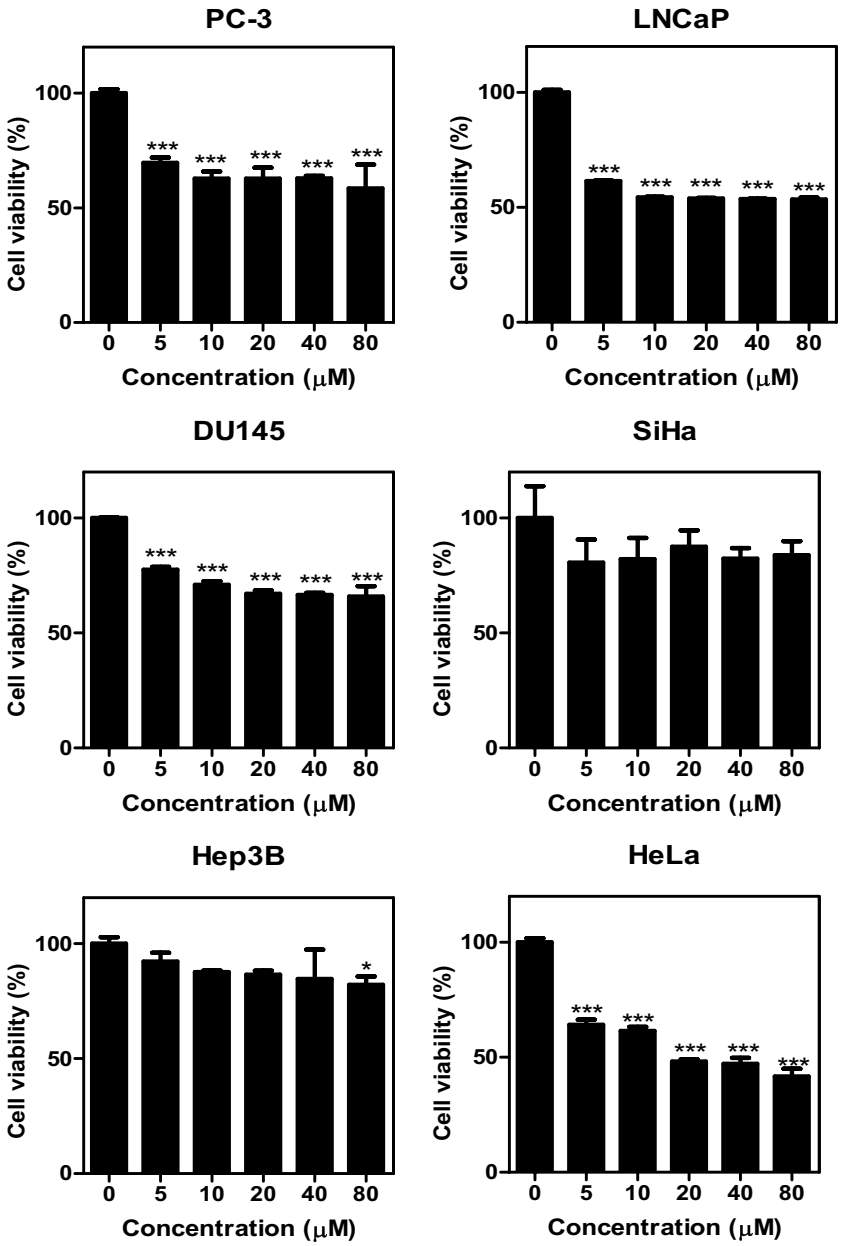

Fig. 9 The cytotoxicity of the identified compound against different prostrate and cervical cancer cells. Cell viability was evaluated by MTT assay. Data represent means ± SDs. *p <.05, ***p <.001

cluster representative in orange indicates the upward movement of the αB helix and downward movement of the αC helix, which might disturb allosteric communication to the ATP site. Allosteric activators generally bind in the PIF pocket and stabilize the ATP binding site to enhance the catalytic activity of PDK1, and allosteric inhibitors binding to the PIF pocket cause the realignment of helices αB and αC in the inactive open conformation, leading to the inhibition of PDK1 activity. This was also supported by the calculated free energy landscape in which the two observed minima were in the open state with highly disturbed αB and αC helices. The upward movement of the αB helix and the downward shifting of the αC helix and well-populated open structures in two energy minima in the free energy surface predicted the identified hit compound to be an allosteric inhibitor. The detailed allosteric mechanism of disrupting PPI binding or inducing conformational changes in the ATP site can be further confirmed by appropriate biological assays. However, these computational studies have proven that the identified compound can very well act as an allosteric modulator of PDK1. These findings provide further evidence that the carboxylic acid moiety is not very essential for an allosteric modulator and that the negative charge might arise from deprotonation of any group present in the

chemical entity. This study serves as an example and can be implicated in future studies of PDK1 as well as other kinases for drug design.

Biological activity

Cervical and prostrate cells were reported to express a significantly high amount of PDK1 (The Human Protein Atlas). Hence, the identified hit compound was tested against three standard prostate cancer cells (PC3, LNCaP, DU145) as well as liver (Hep3B), uterine tissue (SiHa), and HeLa cervical cancer cells. The results indicated that the viability of LNCaP cells was more affected by the addition of the identified compound (Fig. 9). The significant activity of the compound was also found in HeLa cells in a dose-dependent manner. The IC50 value of the compound was found to be 20 µM for HeLa and LNCaP cells. These results imply the anticancer potential of the hit compound at relatively high concentrations in these cell lines when compared to recently reported XAV939 of 10 µM [37] and other marketed drugs like docetaxel (9 µM) against HeLa cells [38].

Most of the compounds exert their activity by apoptosis through intrinsic or extrinsic pathways [39]. To confirm the apoptosis-inducing effects of the hit compound, the expression levels of apoptosis-related proteins in PC-3 cells and LNCaP cells were measured via western blotting after incubation with various doses of the compound for 24 h. Treatment with the compound downregulated caspase-3 and upregulated PARP in LNCaP cells, implying caspase-dependent apoptosis (Fig. S3a). The compound-treated PC-3 cells were further analyzed for inhibition against cell motility-related proteins such as cadherin and vimentin with their antibodies by western blotting. E-cadherin was upregulated (Fig. S3b), and there was no change in the expression of other proteins.

ROS levels in PC-3 cells treated with the compound were also investigated and found to be increased by approximately 20% at a compound concentration of 80 µM (Fig. S3c). PC-3 and LNCaP prostate cancer cells were also subjected to flow cytometry analysis. The identified hit compound notably increased sub-G1 phase accumulation (Fig. S3d) in LNCaP cells, indicating that the cytotoxicity might occur through apoptosis in these cells. There was no evidence of such an increase in PC-3 cells (Fig. S3e). Collectively, the compound was found to have moderate activity at a relatively higher concentration in prostate cancer cells LNCaP and HeLa cervical cells when compared to the available drugs. Thus, there is a need for further modification in the derivational substitutions of the compound. Although the detailed mechanism of interaction of the compound with PDK1 requires additional mediated pathway studies, the substitutional finetuning of the molecule identified is planned for future work.

Conclusions

PDK1 is overexpressed and deregulated in many human solid tumors and not in normal tissues. The disruption of PDK1 interaction with downstream enzymes in the cell signaling pathway constitutes a therapeutic option for cancers. PDK1 targeting has gained importance over the past two decades, and thus far, only a few allosteric modulators have been identified. The need for allosteric modulators of PDK1 still exists in the drug design arena. To this end, we have developed an energy-based pharmacophore model based on the hotspot residues in the protein–protein interaction site of PDK1 to efficiently identify a new scaffold by screening a library of allosteric compounds. The model was validated by enrichment with actives and decoys. The virtual screen workflow further ended up with a new scaffold from the Enamine allosteric library, which is predicted to bind in the PPI site with strong binding affinity with salt bridges, hydrogen bonds, water bridges, and hydrophobic interactions with the key residues of PDK1. The free energy landscape from the metadynamics of the PDK1-ligand complex further confirmed the allosteric effect of the identified compound on the protein. The moderate cytotoxic activity at 20 µM against the LNCaP and PC3 cancer cell lines further supports taking up the identified molecule to fine-tune for becoming a drug candidate against PDK1.

Supplementary Information The online version contains supplementary material available at https://doi.org/10.1007/s00894-024-05842-2.

Acknowledgements KNV greatly acknowledges the Council for Scientific and Industrial Research (CSIR), Govt. of India for a Senior Research Associate fellowship through the Scientists' Pool scheme. The authors also acknowledge Prof. Sung-Hoon Kim's laboratory, College of Korean Medicine, Kyunghee University, South Korea, for all the in vitro studies.

Author contributions Both authors equally contributed to the work and approved the final version of the manuscript.

Declarations

Competing interests The authors declare no competing interests.

References

1. Shekawat SS, Ghosh I (2011) Split-protein systems: beyond binary protein-protein interactions. Curr Opin Chem Biol 15(6):789–797. https://doi.org/10.17159/tvl.v.53i2.27
2. Bakail M, Ochsenbein F (2016) Targeting protein-protein interactions, a wide-open field for drug design. C R Chim 19(1–2):19–27. https://doi.org/10.1016/j.crci.2015.12.004
3. Cossar PJ, Lewis PJ, McCluskey A (2020) Protein-protein interactions as antibiotic targets: a medicinal chemistry perspective. Med Res Rev 40(2):469–494. https://doi.org/10.1002/med.21519

4. Jin L, Wang W, Fang G (2014) Targeting protein-protein interactions by small molecules. Annu Rev Pharmacol Toxicol 54:435–456. https://doi.org/10.1007/978-981-13-0773-7
5. Wang X, Ni D, Liu Y, Lu S (2021) Rational design of peptide-based inhibitors disrupting protein-protein interactions. Front Chem 9(May):1–15. https://doi.org/10.3389/fchem.2021.682675
6. Marondedze EF, Govender KK, Govender PP (2020) Ligand-based pharmacophore modelling and virtual screening for the identification of amyloid-beta diagnostic molecules. J Mol Graph Model 101:107711. https://doi.org/10.1016/j.jmgm.2020.107711
7. Abell C, Scott DE, Ehebauer MT, Pukala T, Marsh M, Blundell TL, Venkitaraman AR, Hyvönen M (2013) Using a fragment-based approach to target protein-protein interactions. ChemBioChem 14(3):332–342. https://doi.org/10.1002/cbic.201200521
8. Petta I, Lievens S, Libert C, Tavernier J, De Bosscher K (2016) Modulation of protein-protein interactions for the development of novel therapeutics. Mol Ther 24(4):707–718. https://doi.org/10.1038/mt.2015.214
9. Souers AJ, Leverson JD, Boghaert ER, Ackler SL, Catron ND, Chen J, Dayton BD, Ding H, Enschede SH, Fairbrother WJ, Huang DCS, Hymowitz SG, Jin S, Khaw SL, Kovar PJ, Lam LT, Lee J, Maecker HL, Marsh KC et al (2013) ABT-199, a potent and selective BCL-2 inhibitor, achieves antitumor activity while sparing platelets. Nat Med 19(2):202–208. https://doi.org/10.1038/nm.3048
10. Gagliardi PA, Puliafito A, Primo L (2018) PDK1: at the crossroad of cancer signaling pathways. Semin Cancer Biol 48:27–35. https://doi.org/10.1016/j.semcancer.2017.04.014
11. Harris TK (2003) PDK1 and PKB/Akt: ideal targets for development of new strategies to structure-based drug design. IUBMB Life 55(3):117–126. https://doi.org/10.1080/1521654031000115951
12. Najafov A, Sommer EM, Axten JM, Deyoung MP, Alessi DR (2011) Characterization of GSK2334470, a novel and highly specific inhibitor of PDK1. Biochem J 433(2):357–369. https://doi.org/10.1042/BJ20101732
13. Biondi RM, Komander D, Thomas CC, Lizcano JM, Deak M, Alessi DR, van Aalten DMF (2002) High resolution crystal structure of the human PDK1 catalytic domain defines the regulatory phosphopeptide docking site. EMBO J 21(16):4219–4228. https://doi.org/10.1093/emboj/cdf437
14. Xu X, Chen Y, Fu Q, Ni D, Zhang J, Li X, Lu S (2019) The chemical diversity and structure-based discovery of allosteric modulators for the PIF-pocket of protein kinase PDK1. J Enzyme Inhib Med Chem 34(1):361–374. https://doi.org/10.1080/14756366.2018.1553167
15. Arkin MMR, Wells JA (2004) Small-molecule inhibitors of protein-protein interactions: progressing towards the dream. Nat Rev Drug Discov 3(4):301–317. https://doi.org/10.1038/NRD1343
16. Rettenmaier TJ, Sadowsky JD, Thomsen ND, Chen SC, Doak AK, Arkin MR, Wells JA (2014) A small-molecule mimic of a peptide docking motif inhibits the protein kinase PDK1. Proc Natl Acad Sci 111(52):18590–18595. https://doi.org/10.1073/pnas.1415365112
17. Arkin MR, Tang Y, Wells JA (2014) Small-molecule inhibitors of protein-protein interactions: progressing toward the reality. Chem Biol 21(9):1102–1114. https://doi.org/10.1016/j.chembiol.2014.09.001
18. Engel M, Hindie V, Lopez-Garcia LA, Stroba A, Schaeffer F, Adrian I, Imig J, Idrissova L, Nastainczyk W, Zeuzem S, Alzari PM, Hartmann RW, Piiper A, Biondi RM (2006) Allosteric activation of the protein kinase PDK1 with low molecular weight compounds. EMBO J 25(23):5469–5480. https://doi.org/10.1038/sj.emboj.7601416
19. Schulze JO, Saladino G, Busschots K, Neimanis S, Süß E, Odadzic D, Zeuzem S, Hindie V, Herbrand AK, Lisa MN, Alzari PM, Gervasio FL, Biondi RM (2016) Bidirectional allosteric communication between the ATP-binding site and the regulatory PIF pocket in PDK1 protein kinase. Cell Chemical Biology 23(10):1193–1205. https://doi.org/10.1016/j.chembiol.2016.06.017
20. Sestito S, Rapposelli S (2019) A patent update on PDK1 inhibitors (2015-present). Expert Opin Ther Pat 29(4):271–282. https://doi.org/10.1080/13543776.2019.1597852
21. Sadowsky JD, Burlingame MA, Wolan DW, McClendon CL, Jacobson MP, Wells JA (2011) Turning a protein kinase on or off from a single allosteric site via disulfide trapping. Proc Natl Acad Sci U S A 108(15):6056–6061. https://doi.org/10.1073/pnas.1102376108
22. Beekman AM, Cominetti MMD, Walpole SJ, Prabhu S, O'Connell MA, Angulo J, Searcey M (2019) Identification of selective protein-protein interaction inhibitors using efficient: in silico peptide-directed ligand design. Chem Sci 10(16):4502–4508. https://doi.org/10.1039/c9sc00059c
23. Gonzalez-Ruiz D, Gohlke H (2006) Targeting protein-protein interactions with small molecules: challenges and perspectives for computational binding epitope detection and ligand finding. Curr Med Chem 13(22):2607–2625. https://doi.org/10.2174/092986706778201530
24. Li B, Rong D, Wang Y (2019) Targeting protein-protein interaction with covalent small-molecule inhibitors. Curr Top Med Chem 19(21):1872–1876
25. Sable R, Jois S (2015) Surfing the protein-protein interaction surface using docking methods: application to the design of PPI inhibitors. Molecules 20(6):11569–11603. https://doi.org/10.3390/molecules200611569
26. Sarvagalla S, Cheung CHA, Tsai JY, Hsieh HP, Coumar MS (2016) Disruption of protein-protein interactions: hot spot detection, structure-based virtual screening and: In vitro testing for the anti-cancer drug target-survivin. RSC Adv 6(38):31947–31959. https://doi.org/10.1039/c5ra22927h
27. Cohen P, Cross D, Jänne PA (2021) Kinase drug discovery 20 years after imatinib: progress and future directions. Nat Rev Drug Discov 20(7):551–569. https://doi.org/10.1038/s41573-021-00195-4
28. Dixon SL, Smondyrev AM, Rao SN (2006) PHASE: a novel approach to pharmacophore modeling and 3D database searching. Chem Biol Drug Des 67(5):370–372. https://doi.org/10.1111/j.1747-0285.2006.00384.x
29. Schrödinger Release 2017-1: Phase, Schrödinger, LLC, New York, NY, 2017
30. Desmond Molecular Dynamics System, D. E. Shaw Research, New York, NY (2021) Maestro-Desmond interoperability tools. Schrödinger, New York, NY, p 2021
31. Li G, Wang Z, Chong T, Yang J, Li H, Chen H (2017) Curcumin enhances the radiosensitivity of renal cancer cells by suppressing NF-κB signaling pathway. Biomed Pharmacother 94:974–981. https://doi.org/10.1016/J.BIOPHA.2017.07.148
32. Rettenmaier TJ, Fan H, Karpiak J, Doak A, Sali A, Shoichet BK, Wells JA (2015) Small-molecule allosteric modulators of the protein kinase PDK1 from structure-based docking. J Med Chem 58(20):8285–8291. https://doi.org/10.1021/acs.jmedchem.5b01216
33. Liu W, Li P, Mei Y (2019) Discovery of SBF1 as an allosteric inhibitor targeting the PIF-pocket of 3-phosphoinositide-dependent protein kinase-1. J Mol Model 25(7). https://doi.org/10.1007/s00894-019-4069-5

34. Wang J, Peng C, Yu Y, Chen Z, Xu Z, Cai T et al (2020). Biophys J 118:1009
35. Stroba A, Schaeffer F, Hindie V, Lopez-Garcia L, Adrian I, Fröhner W et al (2009). J Med Chem 52:4683
36. Busschots K, Lopez-Garcia LA, Lammi C, Stroba A, Zeuzem S, Piiper A et al (2012). Chem Biol 19:1152
37. Stakheev D, Taborska P, Strizova Z, Podrazil M, Bartunkova J, Smrz D (2019). Sci Rep 9(1):4761
38. Altamimi AS, El-Azab AS, Abdelhamid SG, Alamri MA, Bayoumi AH, Alqahtani SM, Alabbas AB, Altharawi AI, Alossaimi MA, Mohamed MA (2021). Molecules 26(10):2992
39. Chen S, Ye H, Gong F, Mao S, Li C, Xu B, Ren Y, Yu R (2021). Oncol Rep 45(4):38

Publisher's Note Springer Nature remains neutral with regard to jurisdictional claims in published maps and institutional affiliations.

Springer Nature or its licensor (e.g. a society or other partner) holds exclusive rights to this article under a publishing agreement with the author(s) or other rightsholder(s); author self-archiving of the accepted manuscript version of this article is solely governed by the terms of such publishing agreement and applicable law.